AD-A260 599

REPORT DOCUMENTATION PAGE

Form Approved
OBM No. 0704-0188

1. Agency Use Only *(Leave blank).*

2. Report Date.
1993

3. Report Type and Dates Covered.
Final - Proceedings

4. Title and Subtitle.
The Construction of Shell Theories with Fluid Loading to Approximate Scattering from Submerged Bounded Objects via Techniques in a Differential Geometry

5. Funding Numbers.
Contract
Program Element No. 0601153N
Project No. 03202
Task No. 350
Accession No. DN255011
Work Unit No. 12211B

6. Author(s).
Cleon E. Dean and Michael F. Werby

7. Performing Organization Name(s) and Address(es).
Naval Research Laboratory Detachment
Ocean Acoustics and Technology Directorate
Stennis Space Center, MS 39529-5004

8. Performing Organization Report Number.
PR 91:134:221

9. Sponsoring/Monitoring Agency Name(s) and Address(es).
Naval Research Laboratory Detachment
Ocean Acoustics and Technology Directorate
Stennis Space Center, MS 39529-5004

10. Sponsoring/Monitoring Agency Report Number.
PR 91:134:221

11. Supplementary Notes.
Published in Computational Acoustics, IMACS.

12a. Distribution/Availability Statement.
Approved for public release; distribution is unlimited.

12b. Distribution Code.

13. Abstract *(Maximum 200 words).*

One can predict sound scattering from fluid loaded elastic shells based on exact elastodynamic theory provided the shell is a sphere or an infinite cylinder or some other geometry for which the elastodynamic equations are separable. Problems arise for more general shapes with only limited success for spheroids and cylinders with hemispherical end caps using the Extended Boundary Condition (EBC) method of Waterman. Both Radlinsky and the Varadans have employed a marriage of the EBC method with shell theories with some progress being made in the description of the scattering event. With this in mind, our objective is to extend the progress made by the above researchers by employing more physical shell theories. It is usual to construct shell theories via use of geometrical constructions, or by use of variational principles. In this study we explore the use of principles from differential geometry to construct appropriate theories that include translational motion and rotary inertia, as well as effects due to fluid loading. Some common thin shell theories which are employed for spherical elastic shells are deduced from these general terms and are compared to exact theory for verification as well as a test of limitations.

14. Subject Terms.
Acoustic scattering, shallow water, waveguide propagation

15. Number of Pages.
15

16. Price Code.

17. Security Classification of Report.	**18. Security Classification of This Page.**	**19. Security Classification of Abstract.**	**20. Limitation of Abstract.**
Unclassified	Unclassified	Unclassified	SAR

Computational Acoustics – Volume I
R.L. Lau, D. Lee and A.R. Robinson (Editors)
Elsevier Science Publishers B.V. (North-Holland)
1993 IMACS

The Construction of Shell Theories with Fluid Loading to Approximate Scattering from Submerged Bounded Objects via Techniques in Differential Geometry

Cleon E. Dean and Michael F. Werby
Naval Oceanographic and Atmospheric Research Laboratory
Numerical Modeling Division
Stennis Space Center, Mississippi 39529-5004

Abstract: One can predict sound scattering from fluid loaded elastic shells based on exact elastodynamic theory provided the shell is a sphere or an infinite cylinder or some other geometry for which the elastodynamic equations are separable. Problems arise for more general shapes with only limited success for spheroids and cylinders with hemispherical end caps using the Extended Boundary Condition (EBC) method of Waterman. Both Radlinsky and the Varadans have employed a marriage of the EBC method with shell theories with some progress being made in the description of the scattering event. With this in mind, our objective is to extend the progress made by the above researchers by employing more physical shell theories. It is usual to construct shell theories via use of geometrical constructions, or by use of variational principles. In this study we explore the use of principles from differential geometry to construct appropriate theories that include translational motion and rotary inertia, as well as effects due to fluid loading. Some common thin shell theories which are employed for spherical elastic shells are deduced from these general terms and are compared to exact theory for verification as well as a test of limitations.

1. INTRODUCTION

We use the standard assumptions of shell theory as formulated by A. E. H. Love (Love, 1944) and which are as follows: (1) The thickness of a shell is small compared with the smallest radius of curvature of the shell; (2) The displacement is small in comparison with the shell thickness; (3) The transverse normal stress acting on planes parallel to the shell middle surface is negligible; (4) Fibers of the shell normal to the middle surface remain so after deformation and are themselves not subject to elongation. These assumptions are used in the development of a shell theory for an elastic spherical shell. The objective here is to build shell theories which produce results consistent with the lowest order Lamb modal vibrations, namely the symmetric and antisymmetric modes. Shell theories for infinite cylinders in free space agree reasonably well with exact theory for the lowest two modes. In particular, the symmetric or dilatational mode is easily accounted for by the simplest shell theory; i.e., a membrane theory. Added sophistication does not appear to alter the general results for the symmetric mode. On the other hand, a membrane theory is completely inadequate to describe the antisymmetric or flexural modes. The inclusion of rotary inertia accounts for the lowest order free space flexural mode but gives results which rapidly depart from the exact calculation with increasing mode number and diverge to infinity for large values of size parameter, *ka*, instead of asymptoting to the Rayleigh phase velocity, as expected. Added complication occurs when one incorporates fluid loading in the exact theory; one first of all does not observe the flexural vibrations until one reaches coincidence frequency. Secondly, there are narrow, well defined water-borne waves analogous to Stoneley waves on a flat plate with fluid loading on one side and a vacuum on the other. Ordinary shell theories yield (even) fourth order resonance equations with real resonance frequencies and no odd order frequency terms. Such an equation yields two real resonance frequency roots and does not suppress the lower order flexural modes; i.e., the subcoincidence antisymmetric modes. By employing complex specific acoustic impedances for the fluid loaded shell, we are able to obtain a fourth order resonant frequency condition with odd order terms and complex frequency roots. Our condition allows for suppression of the lower order flexural modes by damping and may also yield additional roots that correspond to water-borne waves. Although our current results are not completely satisfactory, we feel we have taken a step in the right direction since the new expressions allow for two additional roots in accord with the observation of water-borne waves and for the suppression of the lower order flexural or antisymmetric waves through a damping mechanism. We briefly outline our development below.

2. DERIVATION OF EQUATIONS OF MOTION

In spherical shells membrane stresses (proportional to β) predominate over flexural stresses (proportional to β^2) where

$$\beta = \frac{1}{\sqrt{12}}\frac{h}{a}. \tag{2.1}$$

We differ from the standard derivation for the sphere (Junger and Feit, 1986) by retaining all terms of order β^2 in both the kinetic and potential energy parts of the Lagrangian and by considering the resonance frequencies for the fluid loaded case to be complex. We note that this level of approximation will allow us to include the effects of rotary inertia in our shell theory, as well as damping by fluid loading. The parameter β itself is proportional to the radius of gyration of a differential element of the shell and arises from integration through the thickness of the shell in a radial direction. We will use an implicit harmonic time variation of the form $\exp(-i\omega t)$. We begin our derivation by considering a u,v,w axis system on the middle surface of a spherical shell of radius a (measured to mid-shell) with thickness h, as shown in Fig. 1.

2.1 Lagrangian Variational Analysis

Our Lagrangian, L, is

$$L = T - V + W, \tag{2.2}$$

where T is the kinetic energy, V is the potential energy, and W is the work due to the pressure at the surface. The kinetic energy is given by

$$T = \frac{1}{2}\rho_s \int_0^{2\pi}\int_0^{\pi}\int_{-h/2}^{h/2} (\dot{u}_s^2 + \dot{w}_s^2)(a+x)^2 \sin\theta dx d\theta d\phi, \tag{2.3}$$

where the surface displacements are taken to be linear:

$$\dot{u}_s = (1+\frac{x}{a})\dot{u} - \frac{x}{a}\frac{\partial \dot{w}}{\partial \theta}, \tag{2.4}$$

and

$$\dot{w}_s = \dot{w}. \tag{2.5}$$

The motion of the spherical shell is axisymmetric since the sound field is torsionless. Thus there is no motion in the v-direction. Substitution of Eqs. (2.4) and (2.5) into Eq. (2.3), after integration over x and ϕ,

$$T = \pi\rho_s \int_0^\pi \sin\theta[(\frac{h^5}{80a^2} + \frac{h^3}{2} + ha^2)\dot{u}^2 - 2(\frac{h^5}{80a^2} + \frac{h^3}{4})\dot{u}\frac{\partial \dot{w}}{\partial \theta}$$

$$+(\frac{h^5}{80a^2} + \frac{h^3}{12})(\frac{\partial \dot{w}}{\partial \theta})^2 + (\frac{h^3}{12} + ha^2)\dot{w}^2]d\theta, \tag{2.6}$$

or, in terms of β,

$$T = \pi\rho_s ha^2 \int_0^\pi [(1.8\beta^4 + 6\beta^2 + 1)\dot{u}^2 - (3.6\beta^4 + 6\beta^2)\dot{u}\frac{\partial \dot{w}}{\partial \theta}$$

$$+(1.8\beta^4 + \beta^2)(\frac{\partial \dot{w}}{\partial \theta})^2 + (\beta^2 + 1)\dot{w}^2]\sin\theta d\theta, \tag{2.7}$$

where the first and last terms in square brackets in Eq. (2.7) are associated with linear translational kinetic energies and the middle two terms are associated with rotational kinetic energies of an element of the shell.

The potential energy of the shell is

$$V = \frac{1}{2}\int_0^\pi \int_0^{2\pi} \int_{-h/2}^{h/2} (\sigma_{\theta\theta}\varepsilon_{\theta\theta} + \sigma_{\phi\phi}\varepsilon_{\phi\phi})(x+a)^2 \sin\theta dx d\theta d\phi, \tag{2.8}$$

where the nonvanishing components of the strain are

$$\varepsilon_{\theta\theta} = \frac{1}{a}\left(\frac{\partial u}{\partial \theta} + w\right) + \frac{x}{a^2}\left(\frac{\partial u}{\partial \theta} - \frac{\partial^2 w}{\partial \theta^2}\right), \tag{2.9}$$

and

$$\varepsilon_{\phi\phi} = \frac{1}{a}(\cot\theta u + w) + \frac{x}{a^2}\cot\theta\left(u - \frac{\partial w}{\partial \theta}\right), \tag{2.10}$$

and where the nonzero stress components are

$$\sigma_{\theta\theta} = \frac{E}{1-\nu^2}(\varepsilon_{\theta\theta} + \nu\varepsilon_{\phi\phi}), \tag{2.11}$$

and

$$\sigma_{\phi\phi} = \frac{E}{1-\nu^2}(\varepsilon_{\phi\phi} + \nu\varepsilon_{\theta\theta}), \tag{2.12}$$

where E is Young's modulus. By substitution the potential energy becomes

$$V = \frac{1}{2}\int_0^\pi \int_0^{2\pi} \int_{-h/2}^{h/2} \left[\frac{E}{1-\nu^2}\frac{1}{(x+a)^2}\left([(1+\frac{x}{a})\frac{\partial u}{\partial \theta} - \frac{x}{a}\frac{\partial^2 w}{\partial \theta^2} + w^2]\right.\right.$$

$$+\{\cot\theta[(1+\frac{x}{a})u - \frac{x}{a}\frac{\partial w}{\partial \theta}] + w\}^2$$

$$\left.\left.+2\nu\{\cot\theta[(1+\frac{x}{a})u - \frac{x}{a}\frac{\partial w}{\partial \theta}] + w\}\{(1+\frac{x}{a})\frac{\partial u}{\partial \theta} - \frac{x}{a}\frac{\partial^2 w}{\partial \theta^2} + w]\right)\right](x+a)^2 \sin\theta dx d\theta \tag{2.13}$$

which after integration is

$$V = \frac{\pi Eh}{1-\nu^2}\int_0^{\pi}\{(w+\frac{\partial u}{\partial\theta})^2+(w+u\cot\theta)^2+2\nu(w+\frac{\partial u}{\partial\theta})(w+u\cot\theta)$$

$$+\beta^2[(\frac{\partial u}{\partial\theta}-\frac{\partial^2 w}{\partial\theta^2})^2\cot^2\theta(u-\frac{\partial w}{\partial\theta})^2+2\nu\cot\theta(u-\frac{\partial w}{\partial\theta})(\frac{\partial u}{\partial\theta}-\frac{\partial^2 w}{\partial\theta^2})]\}\sin\theta d\theta. \quad (2.14)$$

Terms in the potential energy proportional to β^2 are due to bending stresses.

And finally, the work done by the pressure of the surrounding fluid on the spherical shell is given by

$$W = 2\pi a^2\int_0^{\pi} p_a w\sin\theta d\theta, \quad (2.15)$$

where p_a is the pressure at the surface.

2.2 The Lagrangian Density and Its Equations of Motion

Integration along the polar angle θ is intrinsic to the problem, therefore we must turn to a *Lagrangian density* formulation to solve for the equations of motion. Our Lagrangian density is just

$$\mathcal{L} = \pi\rho_s ha^2[(1+6\beta^2+1.8\beta^4)\dot{u}^2-(6\beta^2+3.6\beta^4)\dot{u}\frac{\partial\dot{w}}{\partial\theta}+(\beta^2+1.8\beta^4)(\frac{\partial\dot{w}}{\partial\theta})^2$$

$$+(1+\beta^2)\dot{w}^2]\sin\theta-\frac{\pi Eh}{1-\nu^2}\{(w+\frac{\partial u}{\partial\theta})^2+(w+u\cot\theta)^2+2\nu(w+\frac{\partial u}{\partial\theta})(w+u\cot\theta)$$

$$+\beta^2[(\frac{\partial u}{\partial\theta}-\frac{\partial^2 w}{\partial\theta^2})^2+\cot^2\theta(u-\frac{\partial w}{\partial\theta})^2+2\nu\cot\theta(u-\frac{\partial w}{\partial\theta})(\frac{\partial u}{\partial\theta}-\frac{\partial^2 w}{\partial\theta^2})]\}\sin\theta$$

$$+2\pi a^2 p_a w\sin\theta, \quad (2.16)$$

with corresponding differential equations

$$0=\frac{\partial\mathcal{L}}{\partial u}-\frac{d}{d\theta}\frac{\partial\mathcal{L}}{\partial u_\theta}-\frac{d}{dt}\frac{\partial\mathcal{L}}{\partial u_t}, \quad (2.17)$$

and

$$0=\frac{\partial\mathcal{L}}{\partial w}-\frac{d}{d\theta}\frac{\partial\mathcal{L}}{\partial w_\theta}-\frac{d}{dt}\frac{\partial\mathcal{L}}{\partial w_t}+\frac{d^2}{d\theta dt}\frac{\partial\mathcal{L}}{\partial w_{\theta t}}+\frac{d^2}{d\theta^2}\frac{\partial\mathcal{L}}{\partial w_{\theta\theta}}, \quad (2.18)$$

where subscripts denote differentiation of the variable with respect to the subscript.

By substitution of Eqs. (2.17) and (2.18) into (2.16) we obtain

$$0=(1+\beta^2)\left[\frac{\partial^2 u}{\partial\theta^2}+\cot\theta\frac{\partial u}{\partial\theta}-(\nu+\cot^2\theta)u\right]-\beta^2\frac{\partial^3 w}{\partial\theta^3}-\beta^2\cot\theta\frac{\partial^2 w}{\partial\theta^2} \quad (2.19)$$

$$+[(1+\nu)+\beta^2(\nu+\cot^2\theta)]\frac{\partial w}{\partial\theta}-\frac{a^2}{c_p^2}[(1.8\beta^4+6\beta^2+1)\frac{\partial^2 u}{\partial t^2}-(1.8\beta^4+3\beta^2)\frac{\partial^3 w}{\partial\theta\partial t^2}],$$

and

$$-p_a \frac{(1-\nu^2)a^2}{Eh} = \beta^2 \frac{\partial^3 u}{\partial \theta^3} + 2\beta^2 \cot\theta \frac{\partial^2 u}{\partial \theta^2} - [(1+\nu)(1+\beta^2) + \beta^2 \cot^2\theta)] \frac{\partial u}{\partial \theta}$$
$$+\cot\theta[(2-\nu+\cot^2\theta)\beta^2 - (1+\nu)]u - \beta^2 \frac{\partial^4 w}{\partial \theta^4} - 2\beta^2 \cot\theta \frac{\partial^3 w}{\partial \theta^3}$$
$$+\beta^2(1+\nu+\cot^2\theta)\frac{\partial^2 w}{\partial \theta^2} - \beta^2 \cot\vartheta(2-\nu+\cot^2\theta)\frac{\partial w}{\partial \theta} - 2(1+\nu)w$$
$$+\frac{a^2}{c_p^2}[-(1.8\beta^4 + 3\beta^2)\frac{\partial^3 u}{\partial\theta\partial t^2} - (1.8\beta^4 + 3\beta^2)\cot\theta \frac{\partial^2 u}{\partial t^2}$$
$$+(1.8\beta^4 + \beta^2)\frac{\partial^4 w}{\partial\theta^2\partial t^2} + (1.8\beta^4 + \beta^2)\frac{\partial^3 w}{\partial\theta\partial t^2}\cot\theta - (\beta^2+1)\frac{\partial^2 w}{\partial t^2}. \tag{2.20}$$

These differential equations of motion (2.19) and (2.20) have solutions of the form

$$u(\eta) = \sum_{n=0}^{\infty} U_n (1-\eta^2)^{1/2} \frac{dP_n}{d\eta}, \tag{2.21}$$

and

$$w(\eta) = \sum_{n=0}^{\infty} W_n P_n(\eta), \tag{2.22}$$

where $\eta = \cos\theta$ and $P_n(\eta)$ are the Legendre polynomials of the first kind of order n. When the differential equations of motion (2.19) and (2.20) are expanded in terms of Eqs. (2.21) and (2.22), we obtain a set of linear equations in terms of U_n and W_n, whose determinant must vanish. We shall consider two cases: with and without fluid loading.

2.3 Vacuum Case

The simpler case is that when the spherical shell is surrounded by a vacuum such that there is no damping. In this case, the pressure at the surface vanishes: $p_a = 0$. The set of linear equations the expansion coefficients must satisfy are

$$0 = [\Omega^2(1+6\beta^2+1.8\beta^4) - (1+\beta^2)\kappa]U_n + [\Omega^2(3\beta^2+1.8\beta^4) - \beta^2\kappa - (1+\nu)]W_n, \tag{2.23}$$

and

$$0 = -\lambda_n[(\kappa-3)\beta^2 - 1.8\beta^4 + 1 + \nu]U_n + [\Omega^2(1+2\beta^2+1.8\beta^4) - 2(1+\nu) - \beta^2\kappa\lambda_n]W_n, \tag{2.24}$$

where $\Omega = \omega a / c_p$, $\kappa = \nu + \lambda_n - 1$, and $\lambda_n = n(n+1)$. In order for Eqs. (2.23) and (2.24) to be satisfied simultaneously with a non-trivial solution the determinant of the system must vanish:

$$0 = \Omega^4(1+6\beta^2+1.8\beta^4)(1+2\beta^2+1.8\beta^4)$$
$$+\Omega^2\{(3\beta^2+1.8\beta^4)\lambda_n[(\kappa-3)\beta^2 - 1.8\beta^4 + 1 + \nu]$$
$$-[2(1+\nu) + \beta^2\kappa\lambda_n](1+6\beta^2+1.8\beta^4) - (1+\beta^2)\kappa(1+2\beta^2+1.8\beta^4)\}$$
$$+(1+\beta^2)\kappa[2(1+\nu) + \beta^2\kappa\lambda_n] - \lambda_n[(\kappa-3)\beta^2 - 1.8\beta^4 + 1 + \nu](\beta^2\kappa + 1 + \nu). \tag{2.25}$$

Since there are no damping terms, the shell vibrates theoretically forever. Thus, the normalized frequency Ω can be taken to be real. Equation (2.25) is quadratic in Ω^2, thus we expect two real roots to (2.25) and thus two modes for the motion of the shell. They are the symmetric and antisymmetric modes.

2.4 Fluid Loaded Case

For the fluid loaded case, we must consider a modal expansion of the surface pressure in terms of the specific acoustic impedance z_n. In its most general form this is

$$p(a,\theta,\phi) = \sum_{n=0}^{\infty}\sum_{m=0}^{\infty} z_n \dot{W}_{mn} P_n^m(\cos\theta)\cos m\phi, \tag{2.26}$$

where

$$z_n = i\rho c \frac{h_n(ka)}{h_n'(ka)}. \tag{2.27}$$

The specific acoustic impedance z_n can be split into real and imaginary parts:

$$z_n = r_n - i\omega m_n, \tag{2.28}$$

where

$$r_n = \rho c \,\mathrm{Re}\left\{\frac{i h_n(ka)}{h_n'(ka)}\right\}, \tag{2.29}$$

and

$$m_n = -\frac{\rho c}{\omega}\mathrm{Im}\left\{\frac{i h_n(ka)}{h_n'(ka)}\right\}. \tag{2.30}$$

For the case we are considering of axisymmetric motion, the surface pressure is given by

$$p_a(\theta) = -\sum_{n=0}^{\infty} z_n \dot{W}_n P_n(\cos\theta), \tag{2.31}$$

or

$$p_a(\theta) = -\sum_{n=0}^{\infty}(-i\omega W_n r_n - \omega^2 W_n m_n)P_n(\cos\theta). \tag{2.32}$$

Use of Eq.(2.32) in our set of differential equations of motion(2.19) and (2.20) yields the following set of linear equations for the expansion coefficients in the case of a fluid loaded spherical shell:

$$0 = [\Omega^2(1+6\beta^2+1.8\beta^4)-(1+\beta^2)\kappa]U_n + [\Omega^2(3\beta^2+1.8\beta^4)-\beta^2\kappa-(1+\nu)]W_n, \tag{2.33}$$

and

$$\begin{aligned} 0 = &-\lambda_n[(\kappa-3)\beta^2-1.8\beta^4+1+\nu]U_n \\ &+[\Omega^2(1+\alpha+2\beta^2+1.8\beta^4)-2(1+\nu)+\Omega i\gamma-\beta^2\kappa\lambda_n]W_n, \end{aligned} \tag{2.34}$$

where

$$\alpha = \frac{m_n}{\rho_s h}, \tag{2.35}$$

and

$$\gamma = \frac{a}{h}\frac{r_n}{\rho_s c_p}. \tag{2.36}$$

Again the determinant of Eqs. (2.33) and (2.34) must vanish. However, in this instance the value of Ω must be taken to be complex; the resonances have a width that depends on the damping. The result of setting this determinant to zero is

$$\begin{aligned}0 = {} & \Omega^4(1+6\beta^2+1.8\beta^4)(1+\alpha+2\beta^2+1.8\beta^4)\\ & +\Omega^3 i\gamma(1+6\beta^2+1.8\beta^4)\\ & +\Omega^2\{(3\beta^2+1.8\beta^4)\lambda_n[(\kappa-3)\beta^2-1.8\beta^4+1+\nu]\\ & -[2(1+\nu)+\beta^2\kappa\lambda_n](1+6\beta^2+1.8\beta^4)-(1+\beta^2)\kappa(1+\alpha+2\beta^2+1.8\beta^4)\}\\ & +\Omega[-i\gamma(1+\beta^2)\kappa]\\ & +(1+\beta^2)\kappa[2(1+\nu)+\beta^2\kappa\lambda_n]-\lambda_n[(\kappa-3)\beta^2-1.8\beta^4+1+\nu](\beta^2\kappa+1+\nu). \end{aligned} \tag{2.37}$$

Equation (2.37) has four complex roots. From work with an exact modal solution to the problem, we expect two roots to be associated with the symmetric and antisymmetric modes of the shell. We expect the other two roots to be associated with a water-borne pseudo-Stoneley wave.

3. CONCLUSIONS

The next step is to plot the roots of Eqs. (2.25) and (2.37) to compare the resonances predicted by these models with those given by exact modal expansion solutions. By suppressing α and γ, the model associated with Eq.(2.37) reverts to the vacuum case model associated with Eq.(2.25). Similarly suppression of factors of β in Eq. (2.25) will result in a reversion to a previously derived solution (Junger and Feit, 1986). We may then rank the three different models according to their degree of physicality and compare their results for various relative shell thicknesses against each other and against the exact results of the modal expansion model. We may also consider the limitations of each of the models including the exact solution, as well as those of shell models in general.

By setting the values of α and γ in Eq.(2.37) to zero, we revert the shell theory model to one without fluid loading. Similarly, by setting β to zero as well, the model reverts to a membrane model. These models, fluid loaded, vacuo case, and membrane, are successively less physically sophisticated and give successively less good comparison with exact (modal expansion) results. Starting with the least sophisticated model, we see in Fig. 2 thick spherical steel shell dilatational (symmetric) and flexural (antisymmetric) mode resonances calculated by the membrane model. Here and in the succeeding figures thick means h/a =0.1; thin means h/a=0.01. The shell material is a generic steel with density ρ_s = 7.7 times that of water, shear velocity v_s = 3.24 km/s, and longitudinal velocity v_l = 5.95 km/s. The surrounding fluid is taken to be water with density ρ = 1000 kg/m^3 and sound velocity c_w = 1.4825 km/s. The symmetric mode shows a good comparison between exact and shell theory predictions, but the antisymmetric shell theory results for this approximation compare poorly with the exact flexural results. Note that some symmetric mode resonances were not found by our exact theory algorithm. In Fig. 3 we see thin spherical steel shell dilatational (symmetric) and flexural (antisymmetric) mode resonances calculated by the membrane model. Again there is good comparison between dilatational (symmetric) mode resonances calculated by the two methods, except for the first couple of resonances. Only a few exact flexural resonances were picked up by our algorithm. And again the shell theory flexural (antisymmetric) mode resonances do not asymptote properly with increasing order. In Fig. 4, we have thick spherical steel shell dilational (symmetric) and flexural (antisymmetric) mode resonances calculated by shell theory without fluid loading (vacuum). As in the membrane model the shell theory and exact calculations compare well for the dilational (symmetric) mode resonances. In contrast with the membrane model, however, the exact and shell theory calculations for this model show much better agreement for the flexural (antisymmetric) mode resonances. This model does not include fluid loading, but does include the effects of rotary inertia. The vacuum shell theory flexural mode resonances do not asymptote for large size parameter *ka* to the exact results, however. In Fig. 5, we see thin spherical steel shell dilational (symmetric) and flexural (antisymmetric) mode resonances calculated by shell theory without fluid loading (vacuum). As in the membrane model, the shell theory and exact calculations compare well for the dilational (symmetric) mode resonances except for the first couple of resonances. This vacuum model does not have fluid loading, and has insufficient damping for the first two dilational (symmetric) mode resonances. Again, the flexural (symmetric) mode resonances show roughly the correct behavior, but it is not possible to tell what the asymptotic value of the phase velocity would be for large size parameter on this scale. Next, in Fig. 6, we have a plot of thick spherical steel shell dilational (symmetric) and flexural (antisymmetric) mode resonances calculated by shell theory with fluid loading. As in the vacuum case, as well as for the membrane model, the dilational (symmetric) mode resonances compare well for exact and shell theory methods. The flexural (antisymmetric) mode resonances, as calculated by shell theory with fluid loading, do not appear to have the correct asymptotic limit for large size parameter, although they do exhibit roughly the correct behavior for lower values of *ka*. Finally, in Fig. 7, we see thin spherical steel shell dilational (symmetric) and flexural (antisymmetric) mode resonances calculated by shell theory with fluid loading. The exact and shell theory calculations agree well for the dilational (symmetric) resonances and exhibit a marked improvement for the first several shell theory symmetric mode resonances. This is due to the inclusion of fluid loading in the model. The flexural (antisymmetric) mode resonances show the appropriate behavior on this rather limited size parameter scale.

ACKNOWLEDGMENTS

We wish to thank the Office of Naval Research, the Office of Naval Technology, and NOARL management, including Drs. Chin-Bing, Franchi, and Moseley. Dr. Dean is at NOARL on an ONT Fellowship. This work was funded by NOARL Program Element 61153N, G. Car, Program Manager.

REFERENCES

[1] Junger, M. C., and Feit, D., Sound, Structures, and Their Interaction, 2nd ed., MIT Press, Cambridge, Massachusetts, 1986.

[2] Love, A. E. H., A Treatise on the Mathematical Theory of Elasticity, 4th ed., Dover, New York, 1944.

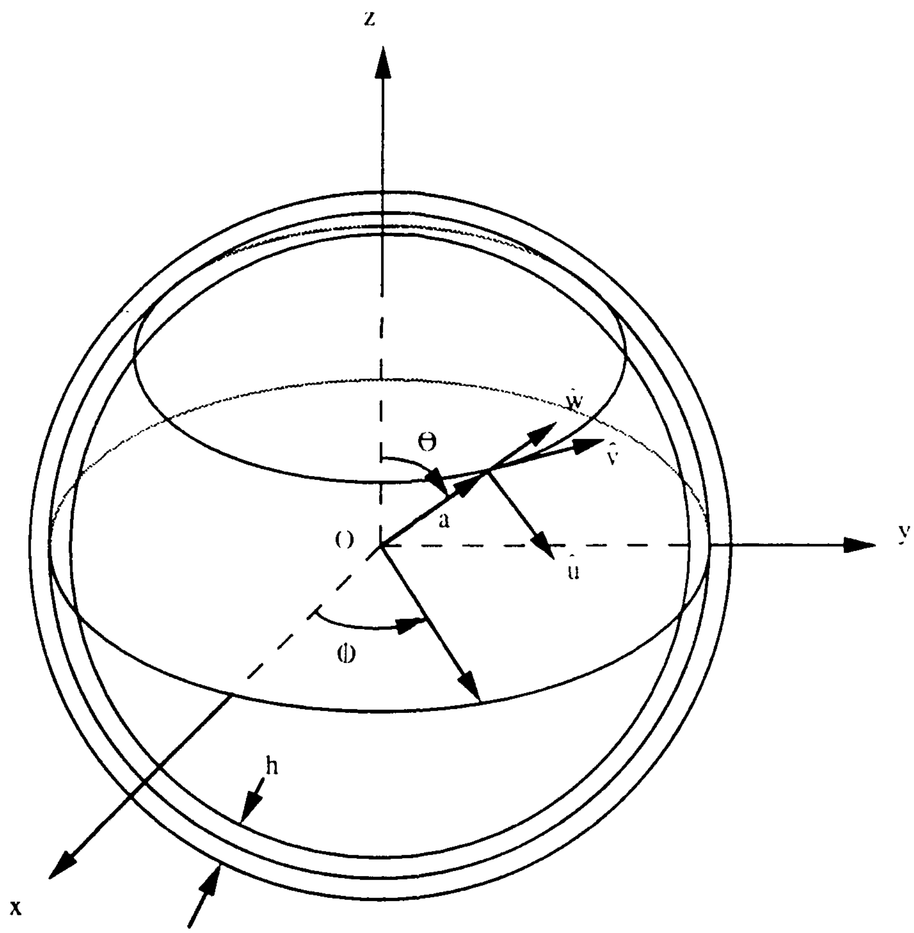

Fig. 1. Spherical shell showing coordinates used.

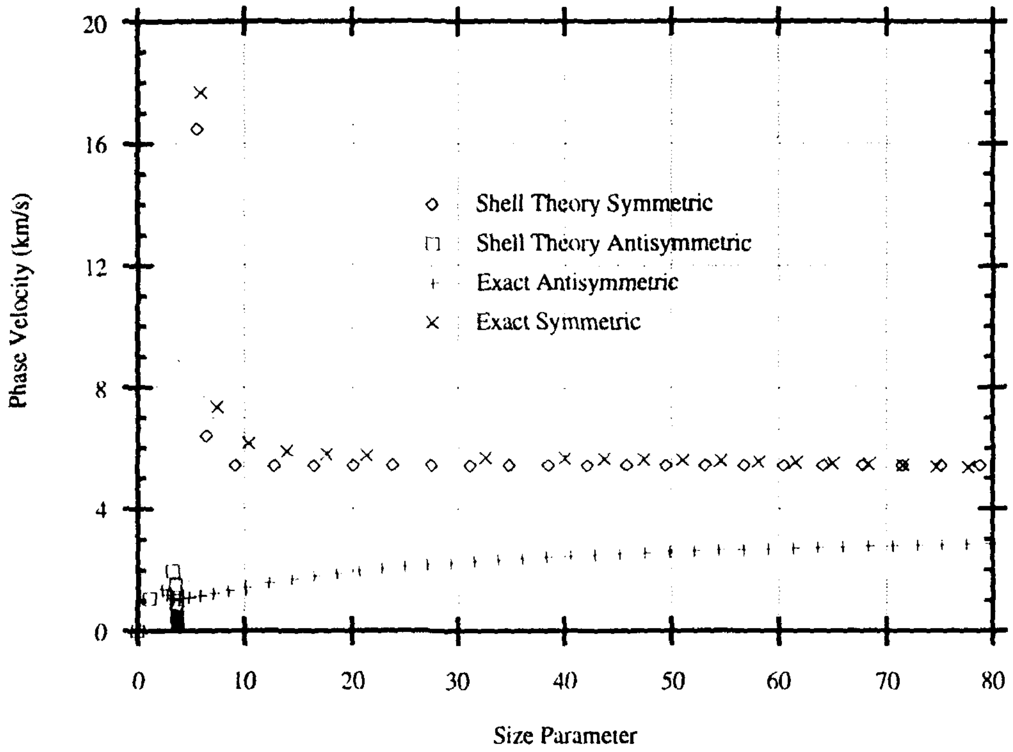

Fig. 2. Thick spherical steel shell dilatational (symmetric) and flexural (antisymmetric) mode resonances calculated by a membrane model. The symmetric mode shows a good comparison between exact and shell theory predictions, but the antisymmetric shell theory results for this approximation compare poorly with the exact flexural results. Some symmetric mode resonances were not found by our exact theory algorithm.

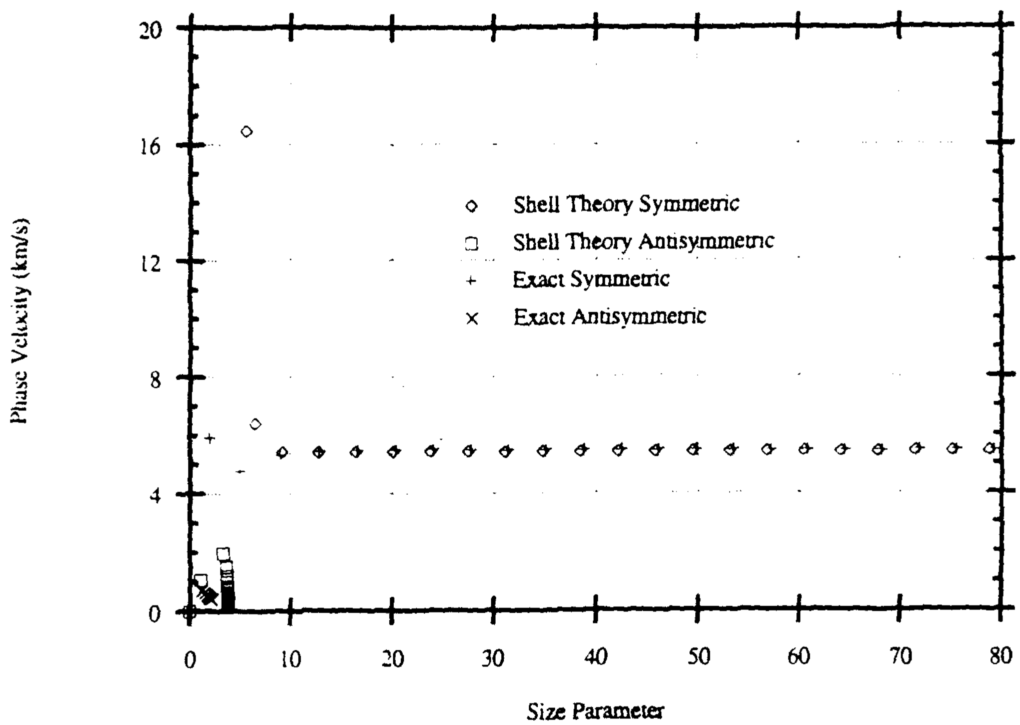

Fig. 3. Thin spherical steel shell dilatational (symmetric) and flexural (antisymmetric) mode resonances calculated by a membrane model. Again there is good comparison between dilatational (symmetric) mode resonances calculated by the two methods, except for the first couple of resonances. Only a few exact flexural resonances were picked up by our algorithm. And again the shell theory flexural (antisymmetric) mode resonances show the wrong behavior with increasing order.

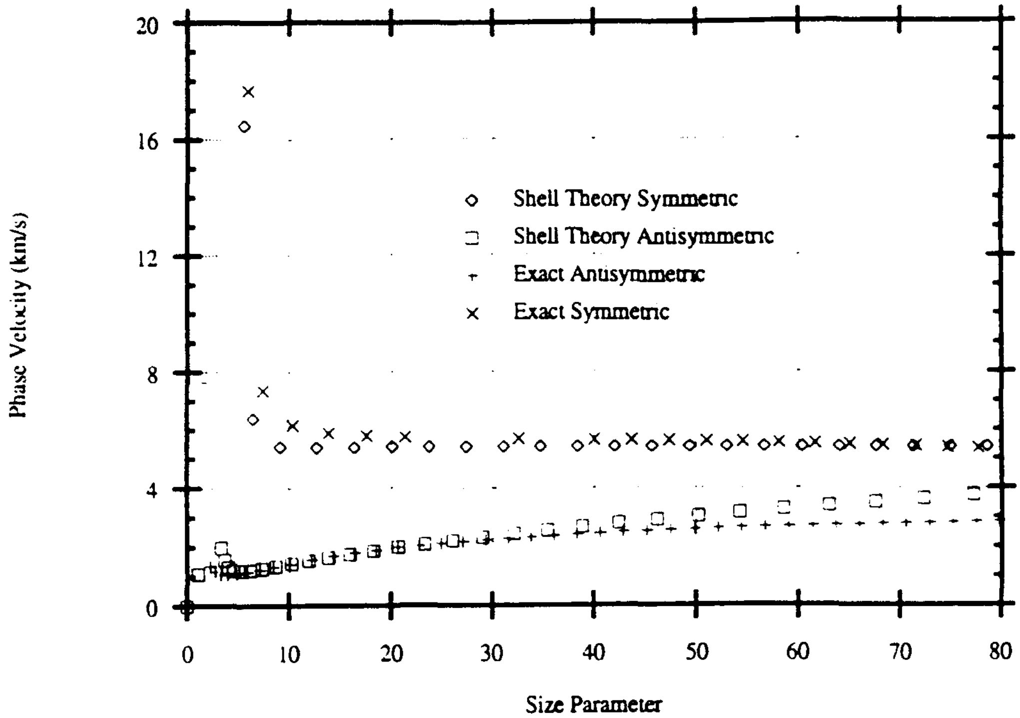

Fig. 4. Thick spherical steel shell dilational (symmetric) and flexural (antisymmetric) mode resonances calculated by shell theory without fluid loading (vacuum). As in the membrane model, the shell theory and exact calculations compare well for the dilational (symmetric) mode resoances. In contrast with the membrane model, however, the exact and shell theory calculations for this model show much better agreement for the flexural (antisymmetric) mode resonances. This model does not include fluid loading, but does include the effects of rotary inertia. The vacuum shell theory flexural mode resonances do not asymptote for large size parameter *ka* to the exact results, however.

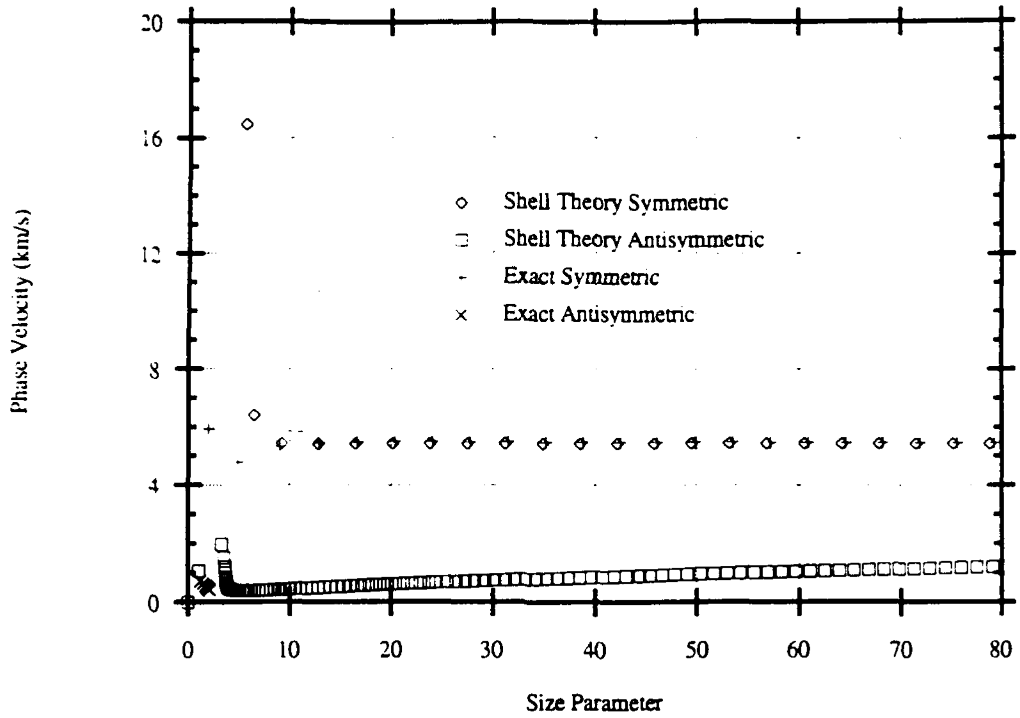

Fig. 5. Thin spherical steel shell dilatational (symmetric) and flexural (antisymmetric) mode resonances calculated by shell theory without fluid loading (vacuum). As in the membrane model the shell theory and exact calculations compare well for the dilatational (symmetric) mode resonances except for the first couple of resonances. This vacuum model does not have fluid loading, and has insufficient damping for the first two dilatational (symmetric) mode resonances. Again, the flexural (symmetric) mode resonances show roughly the correct behavior, but it is not possible to tell what the asymptotic value of the phase velocity would be for large size parameter on this scale.

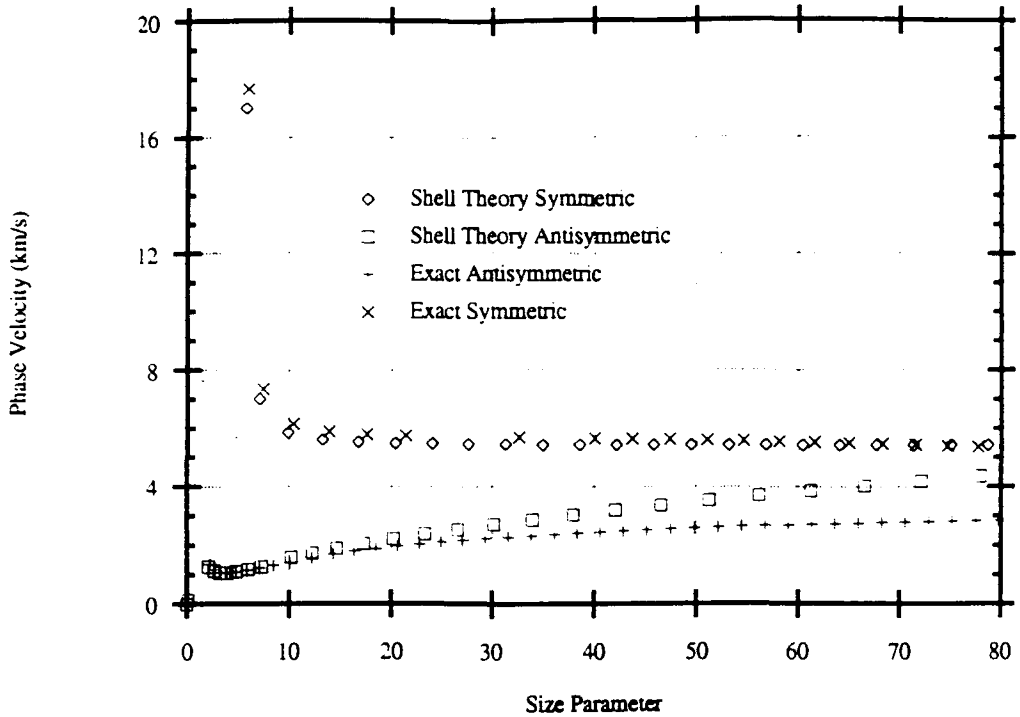

Fig. 6. Thick spherical steel shell dilatational (symmetric) and flexural (antisymmetric) mode resonances calculated by shell theory with fluid loading. As in the vacuum case as well as for the membrane model, the dilatational (symmetric) mode resonances compare well for exact and shell theory methods. The flexural (antisymmetric) mode resonances, as calculated by shell theory with fluid loading, do not appear to have the correct asymptotic limit for large size parameter, although they do exhibit roughly the correct behavior for lower values of *ka*.

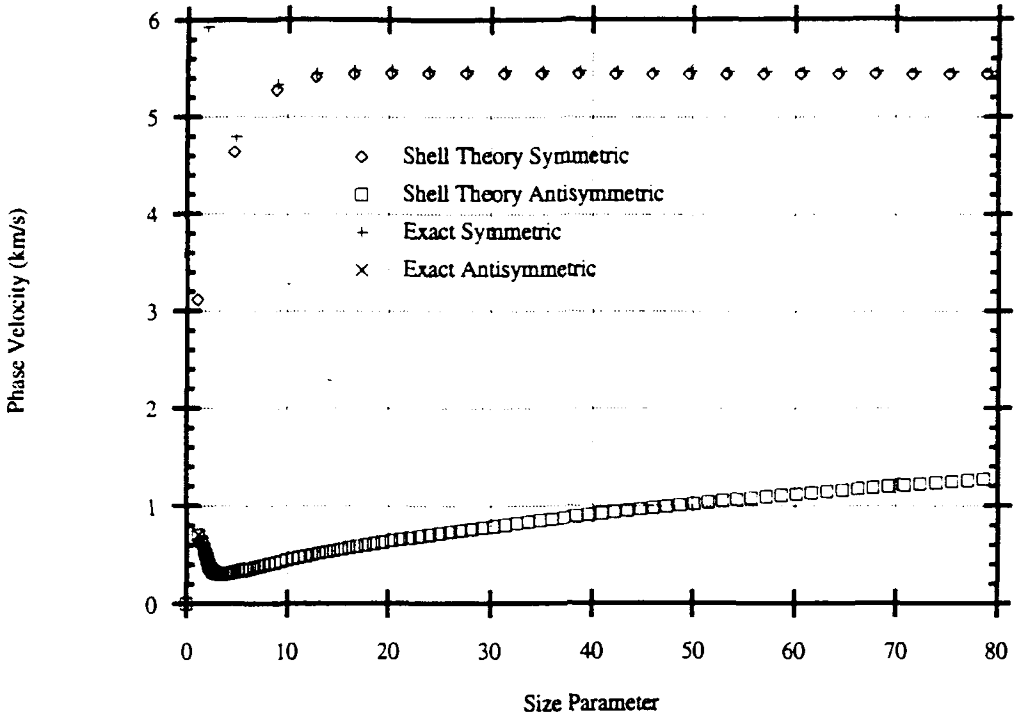

Fig. 7. Thin spherical steel shell dilatational (symmetric) and flexural (antisymmetric) mode resonances calculated by shell theory with fluid loading. The exact and shell theory calculations agree well for the dilatational (symmetric) resonances and exhibit a marked improvement for the first several shell theory symmetric mode resonances. This is due to the inclusion of fluid loading in the model. The flexural (antisymmetric) mode resonances show the appropriate behavior on this rather limited size parameter scale.